Title

Resting-State Functional Connectivity Magnetic Resonance Imaging and Outcome After Acute Stroke.

Journal

Stroke, 49(10)

Authors

Puig, Josep
Blasco, Gerard
Alberich-Bayarri, Angel
et al.

Publication Date

2018-10-01

DOI

10.1161/STROKEAHA.118.021319

Peer reviewed

Published in final edited form as:

Stroke. 2018 October ; 49(10): 2353–2360. doi:10.1161/STROKEAHA.118.021319.

Resting-State Functional Connectivity Magnetic Resonance Imaging and Outcome After Acute Stroke

Josep Puig, MD, **Gerard Blasco, PhD**, **Angel Alberich-Bayarri, PhD**, **Gottfried Schlaug, MD**, **Gustavo Deco, PhD**, **Carles Biarnes, MD**, **Marian Navas-Marti, BS**, **Mireia Rivero, BS**, **Jordi Gich, PhD**, **Jaume Figueras, BS**, **Cristina Torres, BS**, **Pepus Daunis-i-Estadella, PhD**, **Celia L Oramas-Requejo, MD**, **Joaquin Serena, MD**, **Cathy M Stinear, MD**, **Amy Kuceyeski, PhD**, **Carles Soriano-Mas, PhD**, **Götz Thomalla, MD**, **Marco Essig, MD**, **Chase R. Figley, PhD**, **Bijoy Menon, MD**, **Andrew Demchuk, MD**, **Kambiz Nael, MD**, **Max Wintermark, MD**, **David S. Liebeskind, MD**, **Salvador Pedraza, MD**

Imaging Research Unit, Department of Radiology (Girona Biomedical Research Institute) Girona Biomedical Research Institute, Diagnostic Imaging Institute (IDI) (J.R, G.B., C.B., M.N.-M., C.L.O.-R., S.R), Department of Neurology, Girona Biomedical Research Institute (M.R., J.G., J.S.), and Department of Rehabilitation (J.F., C.T.), Dr Josep Trueta University Hospital, Girona, Spain; Quantitative Imaging Biomarkers In Medicine, La Fe Health Research Institute, La Fe Polytechnics and University Hospital, Valencia, Spain (A.A.-B.); Neuroimaging and Stroke Recovery Laboratory, Department of Neurology, Beth Israel Deaconess Medical Center and Harvard Medical School, Boston, MA (G.S.); Center for Brain and Cognition, Universität Pompeu Fabra, Barcelona, Spain (G.D.); ICREA Institut Catalan de Recerca i Estudis Avançais, Barcelona, Spain (G.D.); Department of Computer Science, Applied Mathematics, and Statistics, University of Girona, Spain (P.D.-i.-E.); Department of Medicine, Centre for Brain Research, University of Auckland, New Zealand (C.M.S.); Department of Radiology, Weill Cornell Medical College, NY (A.K.); Department of Psychiatry, Bellvitge University Hospital-Instituto de Investigaciôn Biomédica de Bellvitge, Hospitalet del Llobregat, Barcelona, Spain (C.S.-M.); Centro de Investigaciôn en Salud Mental, Barcelona, Spain (C.S.-M.); and Department of Psychobiology and Methodology in Health Sciences, Universität Autonoma de Barcelona, Spain (C.S.-M.); Department of Neurology, University Medical Centre Hamburg-Eppendorf, Hamburg, Germany (G.T.); Department of Radiology, University of Manitoba, Winnipeg, Canada (M.E., C.R.F.); Departments of Clinical Neurosciences and Radiology, Hotchkiss Brain Institute, University of Calgary, Alberta, Canada (B.M., A.D.); Department of Radiology, Icahn School of Medicine at Mount Sinai, NY (K.N.); Neuroradiology Division, Department of Radiology, Stanford University, Palo Alto, CA (M.W.); and Neurovascular Imaging Research Core and University of California Los Angeles Stroke Center, Los Angeles, CA (D.S.L.).

Abstract

Correspondence to Josep Puig, MD, Department of Radiology-IDIBGI, Av de Francia s/n, Hospital Universitari de Girona Dr Josep Trueta, 17007 Girona, Spain. jpuigalcantara@idibgi.org.

Guest Editor for this article was Georgios Tsivgoulis, MD.

Disclosures

None.

Background and Purpose——Physiological effects of stroke are best assessed over entire brain networks rather than just focally at the site of structural damage. Resting-state functional magnetic resonance imaging can map functional-anatomic networks by analyzing spontaneously correlated low-frequency activity fluctuations across the brain, but its potential usefulness in predicting functional outcome after acute stroke remains unknown. We assessed the ability of resting-state functional magnetic resonance imaging to predict functional outcome after acute stroke.

Methods——We scanned 37 consecutive reperfused stroke patients (age, 69±14 years; 14 females; 3-day National Institutes of Health Stroke Scale score, 6±5) on day 3 after symptom onset. After imaging preprocessing, we used a whole-brain mask to calculate the correlation coefficient matrices for every paired region using the Harvard-Oxford probabilistic atlas. To evaluate functional outcome, we applied the modified Rankin Scale at 90 days. We used region of interest analyses to explore the functional connectivity between regions and graph-computation analysis to detect differences in functional connectivity between patients with good functional outcome (modified Rankin Scale score ≤2) and those with poor outcome (modified Rankin Scale score >2).

Results——Patients with good outcome had greater functional connectivity than patients with poor outcome. Although 3-day National Institutes of Health Stroke Scale score was the most accurate independent predictor of 90-day modified Rankin Scale (84.2%), adding functional connectivity increased accuracy to 94.7%. Preserved bilateral interhemispheric connectivity between the anterior inferior temporal gyrus and superior frontal gyrus and decreased connectivity between the caudate and anterior inferior temporal gyrus in the left hemisphere had the greatest impact in favoring good prognosis.

Conclusions——These data suggest that information about functional connectivity from resting-state functional magnetic resonance imaging may help predict 90-day stroke outcome.

Keywords

brain; magnetic resonance imaging; patients; reperfusion; stroke

Stroke is a leading cause of disability and dependency in adults. In 2010, there were about 11.6 million incident ischemic stroke events in the United States.[1] By 2030, an additional 3.4 million adults will have had strokes.[2] Being able to predict outcome could help patients and caregivers to plan for the future and physicians and policymakers to develop effective rehabilitation plans. Although baseline measures of stroke severity represent the best pretreatment predictors of outcome, other markers of stroke severity, such as change in National Institutes of Health Stroke Scale (NIHSS), infarct volume, 24-hour NIHSS, or 2-day NIHSS trajectory, are the strongest posttreatment predictors of 90-day outcome.[3–5] However, patients' neurological impairment sometimes exceeds what would be expected from stroke magnitude. Stroke lesions not only result in focal, location-dependent neurological symptoms but can also induce widespread effects in remote regions in the affected and unaffected hemispheres connected through functional networks.[6] Although growing evidence emphasizes the role of distributed neural networks in the control of

behavior,[7] Little is known about what patterns of interaction within a functional network are most closely associated with stroke outcome.

Resting-state functional magnetic resonance imaging (rs-fMRI) measures the temporal correlation of variations in blood oxygenation level-dependent signal across brain regions in the absence of imposed tasks, providing a measure of temporal coherence between regions.[8] Recent evidence indicates that functional networks identified by rs-fMRI strongly overlap with networks activated by task performance[9] and that spontaneous activity correlates with trial-to-trial fluctuations in task-evoked responses[10] and behavior.[11] The loss of coherence in spontaneous blood oxygenation level-dependent fluctuations at rest between regions that belong to a functional network, and presumably between different related functional networks, seems to predict behavioral deficits. Some observations point to the importance of interhemispheric connections. For instance, inhibitory influences from the undamaged hemisphere onto the damaged hemisphere decrease during motor recovery,[12] and rebalancing this imbalance is 1 way of improving a patient's outcome.[13] Moreover, after damage to right-hemisphere-dominant neural systems that result in spatial neglect, activation of left and right parietal regions is unbalanced, and interhemispheric functional connectivity in the parietal cortex decreases.[14,15] Furthermore, disruption of functional connectivity between structurally normal left and right posterior parietal regions correlates with the degree of spatial neglect after stroke.[15] However, to date, studies in stroke patients have mainly focused on motor recovery and cognitive outcomes,[1222] and there is little evidence about the impact of functional connectivity on functional outcome after acute stroke.[23] We aimed to investigate the prognostic utility of rs-fMRI by itself and in combination with other predictors at day 3 after stroke symptom onset in predicting 90-day functional outcome and to determine whether a model incorporating information about functional connectivity from rs-fMRI and early markers of stroke severity could predict functional outcome better than clinical scores alone.

Material and Methods0

The data that support the findings of this study are available from the corresponding author on reasonable request.

Patients

This prospective, longitudinal study included consecutive patients aged >18 years admitted to our stroke unit with first-ever supratentorial arterial ischemic stroke between September 2015 and May 2017. All patients modified Rankin Scale (mRS) score before admission was zero, and all underwent clinical follow-up at 90 days. All patients received intravenous r-tPA (recombinant tissue-type plasminogen activator). We excluded patients whose symptoms completely resolved within 72 hours after onset, and those with concomitant neurological disorders, contraindications to MRI (pacemaker, metallic foreign bodies, or severe claustrophobia), or parenchymal hematoma type 2 after fibrinolysis (defined as a space-occupying hematoma filling >30% of the infarct zone with a substantial mass effect), which portends poor prognosis.[24] Middle cerebral artery was monitored during r-tPA perfusion. Stroke severity was defined by the 3-day NIHSS score.[25] Functional outcome at day 90 was

assessed using the mRS; patients with mRS ≤2 were considered functionally independent.[26] All patients were managed according to recent guidelines.[27] Standard rehabilitation programs were initiated once patients were clinically stable. The study was approved by the institutional ethics committee and was conducted in accordance with the Helsinki Declaration. Participants or their relatives provided written informed consent before participating in the study.

Image Acquisition

All scans were acquired on day 3 after symptom onset on a 1.5-T MRI system (Gyroscan Intera; Philips Medical Systems, Best, the Netherlands) with a 16-channel phased-array head coil with foam padding and headphones to restrict head motion and suppress scanner noise. The rs-fMRI was performed by using a gradient echo-planar imaging sequence (repetition time, 2500 ms; echo time, 50 ms; flip angle, 90; voxel size, 2.5×2.5×4 mm without gap and field of view, 24×24 cm), and 240 continuous functional volumes were acquired axially for 10 minutes. Subjects were instructed to relax, keep their eyes closed, stay awake, remain still, and clear their heads of all thoughts. The scan protocol included axial T1-weighted images (repetition time, 8.4 ms; echo time, 4.1 ms; flip angle, 8°; field of view, 230 mm; and voxel size, l×l×l mm) and diffusion tensor imaging. Axial diffusion tensor imaging were acquired in 16 noncollinear diffusion directions, with b-values of 1000 s/mm^2 and 0 s/mm^2, with the following echo-planar acquisition protocol: repetition time, 3148 mm; echo time, 86 ms; flip angle, 90°; field of view, 230 mm; no gap; and voxel size, 2×2×2.5 mm. Fluid-attenuated inversion recovery images (repetition time, 6000 ms; echo time, 140 ms; inversion time, 2200 ms; and voxel size, 0.7×0.7×5 mm) were analyzed by a neuroradiologist with 15 years' experience.

Lesion Analysis

Infarct localization, laterality, and vascular territory involved were determined by MRI on day 3 after symptom onset (Figure 1). Lesion volume was determined by a semi-automated segmentation algorithm applied to axial diffusion-weighted imaging.[28]

Image Preprocessing

The preprocessing pipeline is illustrated in Figure 2; rs-fMRI images were initially processed using SPM8 (Wellcome Trust Center for Neuroimaging, University College London, London, United Kingdom) and the resting-state FC MRI Data Analysis Toolkit.[29] The first steps involved correcting for slice acquisition timing and bulkhead motion. Motion parameters were computed by estimating translation and angular rotation in the *x, y*, and *z* axes. The datasets were excluded if motion was >2 mm (maximum displacement) in *x, y*, or *z* or if angular rotation was >2° within the 4-dimensional volume. New motion variables were generated to be included as covariates in the statistical analysis. To remove the effects of the nuisance covariates, we used linear regression of the global mean signal, white matter signal, and cerebrospinal fluid signal. Spatial normalization was performed using a standard echo-planar imaging template from the Montreal Neurological Institute with a voxel size of 2×2×2 mm^3.[30] Specifically, functional images were coregistered to their corresponding T1-weighted anatomic images using mutual information as an objective function. The anatomic images were then normalized to SPM's Montreal Neurological Institute 2-mm T1 template

by a 12-parameter affine transformation, followed by a nonlinear registration using a mean squared difference matching function. The transformation matrix was applied to normalize all images to the template space. The normalized functional images were then spatially smoothed with a gaussian kernel (full width at half maximum, 8 mm). The temporal signals in the 4-dimensional volume were linearly detrended and band-pass filtered (0.01–0.08 Hz) to remove undesired components. The Harvard-Oxford probabilistic atlas was used to identify the regions of interest (ROI) in the study.[31]

ROI-Based Analyses and Graph-Computation Analysis

For every pairwise region identified with the Harvard-Oxford probabilistic atlas, the correlation coefficients were calculated after removing the nonneural blood oxygenation level-dependent fluctuations. To calculate the ROI-to-ROI correlations, we used automatic low-frequency fluctuation methods,[32] which yielded correlation matrices to show the correlation values as colors and corresponding graphs to enable the matrices to be visualized (CONN V.17, Functional Connectivity SPM toolbox; McGovern Institute of Brain Research, Massachusetts Institute of Technology) to detect differences between patients with good functional versus poor functional outcome. Heatmaps were used to determine the absolute correlation between brain regions. Stronger functional connections were plotted in warmer colors.

Data Analysis

We compared demographic, clinical, and imaging data between patients with good versus poor functional outcome at 90 days. Descriptive statistics are expressed as means (SD) for continuous variables and as frequencies (percentages) for categorical variables. After checking for normality of distributions, the significant ROI-to-ROI relationships were introduced in a discriminant function analysis to uncover the best combination of input variables to differentiate patients' functional outcome (SPSS version 23; IBM).[33] Standardized canonical discriminant function coefficients were used to enable the variables to be measured on the same scale and then the weights were compared to determine the relative importance of each variable. The discriminating variables were also expressed in standard (Z) scores, and these standardized coefficients were used to predict functional outcome at 90 days.

Results

Demographic and Clinical Data

Of 65 consecutive patients, 28 were excluded for absence of symptoms by day 3 (n=9), parenchymal hematoma 2 after fibrinolysis (n=3), excessive motion during fMRI (n=7), pacemakers (n=2), or absence of clinical follow-up at 90 days (n=7). Table 1 describes the demographic and clinical characteristics of the 37 patients (age, 68±13.2 years; 17 females; NIHSS, 6.8±5.6; 100% right-handed) included in the analysis. Figure 2 shows patients' infarcts on axial diffusion weighted imaging. Patients with poor functional outcome had higher 3 day-NIHSS. Age, sex, vascular risk factors, and time to intravenous fibrinolysis were similar between patients with good functional outcome and those with poor outcome.

Functional Connectivity and Functional Outcome

Figure 1 shows the correlation coefficient weighted matrices for every pairwise region in each patient. Patients with good functional outcome had greater functional connectivity than those with poor outcome (Figure 3), including greater interhemispheric connectivity between the right temporal lobe and left frontal lobe, between the left temporal lobe and right frontal lobe and between the right temporal and parietal lobes (Table 2). In addition, patients with good outcome had decreased interhemispheric functional connectivity between the cerebellum and different cerebral nodes, such as the anterior inferior temporal gyrus (alTG), insular cortex, and intracalcarine cortex. Decreased functional connectivity between the alTG and caudate was associated with good outcome (Figure 3). Non-middle cerebral artery distribution strokes did not result in significant differences in the functional connectivity and outcome than the middle cerebral artery territory strokes.

Discriminant Function Analysis

The standardized canonical discriminant function coefficients for age, 3-day NIHSS score, infarct volume, and infarct territory were 0.179, 1.129, −0.318, and −0.064, respectively. Therefore, 3-day NIHSS score had the best discriminating power to predict patients' 90-day stroke outcome. The model, including these 4 variables, predicted functional outcome with 84.2% accuracy. Adding information about functional connectivity from fMRI increased the accuracy to 94.7%. Functional connectivity between the right alTG and left superior frontal gyrus (SFG), left alTG and right SFG, and left alTG and left caudate yielded the highest standardized canonical discriminant function coefficients (ie, had the greatest weight in predicting functional outcome; Table 3).

Discussion

To our knowledge, this is the first study to evaluate the usefulness of functional connectivity measured by rs-fMRI on day 3 after stroke onset in predicting patients' 90-day mRS. Growing evidence supports the conclusion that interhemispheric connectivity affects stroke outcome.[6] Disrupted interhemispheric communication is a central feature of stroke.[12–15] We found that patients with good functional outcome had greater functional connectivity than patients with poor outcome. Preserved connectivity between the alTG and SFG across hemispheres and decreased connectivity between the caudate and alTG in the left hemisphere had the greatest impact on outcome. These results might reflect the structural neuroadaptations taking place in the most severely injured brains. In these brains, interhemispheric connectivity is particularly decreased, which may result in compensatory increases of same-side connectivities, involving cortico-subcortical connections (ie, left caudate with left alTG) and typical crossed connections between the right cerebellum and the left cerebellar hemisphere. In patients with good outcome, such same-side connectivity increases would not be as necessary, and, therefore, decreased functional connectivities between these specific pairs of regions would be observed in comparison to poor outcome patients. Animal studies have revealed profuse intrahemispheric and interhemispheric frontotemporal connections[34,35] and humans have similar strong connections between frontal and temporal lobes (eg, arcuate fasciculus, uncinate fasciculus, extreme capsule fiber tract, and frontal aslant tract). Many projections from the frontal cortex cross the corpus

callosum to connect with heterotopic contralateral areas, as well as with their homotopic counterparts.[36] Preserved interhemispheric functional connectivity, particularly between frontal and temporal regions, might be important in maintaining the brain's ability to recover, as well as possible. However, functional connectivity may decrease as a means of isolating damaged areas rather than because of damage from stroke.[17] However, the physiology underlying reduced interhemispheric functional connectivity after a stroke remains unclear. Structural connections or mechanisms that mediate the transfer of signals between the hemispheres might be damaged or functioning abnormally. Reduced interhemispheric functional connectivity is accompanied by decreases in manganese transfer from the contralesional to the ipsilesional hemisphere,[37] consistent with a reduction in callosal fibers which was shown using decreased fractional anisotropy of the corpus callosum as a surrogate marker in chronic stroke patients.[38] Electroencephalography signals (power, coherence) are abnormal both within and across hemispheres and correlate with behavioral impairment after stroke.[39] Recently, Siegel et al[7] found that lesion load partly predicted the global average reduction in interhemispheric functional connectivity (r=0.46), but adding information about lesion location did not improve predictions. They demonstrated that strokes disrupt interhemispheric functional connectivity regardless of whether they damage specific structures, such as the corpus callosum or thalamus.

Our results are in line with those reported by Dacosta-Aguayo et al,[17] who found bilateral interhemispheric integrity between the ITG and SFG and between the 2 ITGs in stroke patients and controls. They also found that, compared with controls, patients had decreased functional connectivity between the left SFG and posterior cingulate cortex, between the left parahippocampal gyrus and right SFG, between the left parahippocampal gyrus and left SFG, and between the right parietal cortex and left SFG. Other authors have related reduced functional connectivity between the right middle temporal cortex and right SFG and between the left middle temporal cortex and right SFG to memory dysfunction after stroke.[21] Carter et al[16] found that loss of interhemispheric functional connectivity between homologous regions of the dorsal attention network correlated with deficits in patients' ability to detect targets in the visual field contralateral to the lesion. This result generalized to the motor system, where loss of interhemispheric connectivity in an arm-defined somatomotor network correlated with measures of upperlimb function. He et al[15] reported a breakdown of interhemispheric functional connectivity within the attention network in patients with neglect symptoms after stroke; more severe symptoms correlated with decreased functional connectivity, and recovery from symptoms correlated with the recovery of normal connectivity patterns. The integrity of various motor and nonmotor networks (eg, executive control, sensorimotor, visuospatial, and language networks) is associated with stroke outcome,[6,23,40–42] and decreased interhemispheric functional connectivity correlates with increased intrahemispheric functional connectivity between the default mode network and attention network.[7]

We found that 3-day NIHSS score predicted outcome better than other markers of stroke severity, corroborating previous studies' findings that early markers of stroke severity can accurately predict patient outcomes.[3–5] Recently, Sajobi et al[3] found that the trajectory of neurological improvement defined by 2-day longitudinal NIHSS data yielded the most accurate prediction of 90-day mRS (84.5%). Another study concluded that the binary

outcome of NIHSS 0 to 2 at 24 hours was the most powerful predictor of the effect of intravenous thrombolysis.[4] However, variability between individuals makes accurate prognosis for individual patients difficult. Imaging methods have found that the corticospinal tract-lesion load (determined after 24 hours after a stroke) predicts motor outcome, particularly for those patients that are most severely affected.[22] Growing evidence supports that in stroke patients with mild-to-moderate deficits, the degree of initial impairment predicts outcome at 3 months.[43,44] However, in patients with moderate-to-severe acute deficits, high-interindividual variability in recovery makes predicting outcomes much more difficult.[45] In this respect, adding the brain functional connectivity in patients with moderate-to-severe deficits can eventually be used to individually set therapeutic goals and strategies and to select patients for trials.

Several limitations of our study deserve comment. Our small sample limits the generalizability of our results; new and larger samples are necessary to confirm our results. The accuracy and reproducibility of brain network models depend on the regions used. In functional connectivity analysis, which structures are included and how those structures are parcellated are important; the cortical parcellation we chose optimally separates functional connectivity data.[30] Using 3T or 7T system would improve analyses of functional networks. Several experiments at high-magnetic fields have revealed the potential to benefit in terms of sensitivity, specificity, and higher spatial resolution for functional mapping of brain organization from large cortical networks, small nuclei, and even to cellular layer structures.[46,47] We did not analyze possible group differences in vascular risk factors (eg, diabetes mellitus, hypertension, dyslipidemia) that are more frequent in stroke patients and can confound rs-fMRI measurements of fluctuations in functional connectivity either by interfering with the blood oxygenation level-dependent signal or by causing small vessel stroke in periventricular and subcortical white matter locations; for example, patients with diabetes mellitus reportedly have decreased functional connectivity.[42] A recent study found that functional connectivity was better than lesion location at predicting behavioral deficits involving associative functions (eg, memory), but location was better at predicting motor and visual deficits; both approaches predicted language deficits well predicted, and there was a trend for functional connectivity to predict attention deficits better than lesion location.[7] Therefore, functional associations probably depend at least partly on structural connectivity; further work is needed to better elucidate whether combining information about structural and functional connectivity can increase accuracy in predicting stroke outcome. To reduce the patient selection bias, we performed the imaging protocol at day 3 because clinical improvement after reperfusion as well as the residual level of impairment after an acute intervention are robust predictors of outcome, irrespective of initial clinical severity before any reperfusion therapy is initiated.[48]

In conclusion, these results suggest that rs-fMRI information about functional connectivity can complement early markers of stroke severity in predicting patients' 90-day stroke outcome and help stratify patients according to their chance of recovery. Understanding the network changes caused by stroke might enable rehabilitation interventions to be tailored to improve recovery.

Sources of Funding

This work was supported by a grant from the Spanish Ministry of Health, Institute de Investigación Carlos III. REF PI 13/02545 (Desarrollo de un biomarcador radiológico basado en el análisis de la conectividad estructural y funcional en pacientes con infarto cerebral para la predicción de la recuperatión funcional). Dr Soriano-Mas is supported by a Miguel Servet contract (CPU16/00048) from the Carlos III Health Institute.

References

1. Krishnamurthi RV, Feigin VL, Forouzanfar MH, Mensah GA, Connor M, Bennett DA, et al. Global and regional burden of first-ever ischaemic and haemorrhagic stroke during 1990–2010: findings from the Global Burden of Disease Study 2010. Lancet Glob health.2013;l:e259–e281.
2. Mozaffarian D, Benjamin EJ, Go AS, Arnett DK, Blaha MJ, Cushman M, et al. Heart Disease and Stroke Statistics-2016 Update: a report from the American Heart Association. Circulation. 2016;133:e38–360. [PubMed: 26673558]
3. Sajobi TT, Menon BK, Wang M, Lawal O, Shuaib A, Williams D, et al.; ESCAPE Trial Investigators. Early trajectory of stroke severity predicts long-term functional outcomes in ischemic stroke subjects: results from the ESCAPE Trial (Endovascular Treatment for Small Core and Anterior Circulation Proximal Occlusion With Emphasis on Minimizing CT to Recanalization Times). Stroke. 2017;48:105–110. doi: 10.1161/STROKEAHA.116.014456 [PubMed: 27924049]
4. Kerr DM, Fulton RL, Lees KR; VISTA Collaborators. Seven-day NIHSS is a sensitive outcome measure for exploratory clinical trials in acute stroke: evidence from the Virtual International Stroke Trials Archive. Stroke. 2012;43:1401–1403. doi: 10.1161/STROKEAHA.111.644484 [PubMed: 22308254]
5. Broderick JP, Lu M, Kothari R, Levine SR, Lyden PD, Haley EC, et al. Finding the most powerful measures of the effectiveness of tissue plasminogen activator in the NINDS tPA stroke trial. Stroke. 2000;31:2335–2341. [PubMed: 11022060]
6. Grefkes C, Fink GR. Connectivity-based approaches in stroke and recovery of function. Lancet Neurol. 2014;13:206–216. doi: 10.1016/S1474-4422(13)70264-3 [PubMed: 24457190]
7. Siegel JS, Ramsey LE, Snyder AZ, Metcalf NV, Chacko RV, Weinberger K, et al. Disruptions of network connectivity predict impairment in multiple behavioral domains after stroke. Proc Natl Acad Sei USA. 2016;113:E4367–E4376. doi: 10.1073/pnas.l521083113
8. Azeez AK, Biswal BB. A review of resting-state analysis methods. Neuroimaging Clin N Am. 2017;27:581–592. doi: 10.1016/j.nic.2017.06.001 [PubMed: 28985930]
9. Fox MD, Raichle ME. Spontaneous fluctuations in brain activity observed with functional magnetic resonance imaging. Nat Rev Neuro sei. 2007;8:700–711. doi: 10.1038/nrn2201
10. Fox MD, Snyder AZ, Zacks JM, Raichle ME. Coherent spontaneous activity accounts for trial-to-trial variability in human evoked brain responses. Nat Neurosci. 2006;9:23–25. doi: 10.1038/nnl616 [PubMed: 16341210]
11. Fox MD, Snyder AZ, Vincent JL, Raichle ME. Intrinsic fluctuations within cortical systems account for intertrial variability in human behavior. Neuron. 2007;56:171–184. doi: 10.1016/j.neuron.2007.08.023 [PubMed: 17920023]
12. Ward NS, Cohen LG. Mechanisms underlying recovery of motor function after stroke. Arch Neurol. 2004;61:1844–1848. doi: 10.1001/archneur.61.12.1844 [PubMed: 15596603]
13. Lindenberg R, Renga V, Zhu LL, Nair D, Schlaug G. Bihemispheric brain stimulation facilitates motor recovery in chronic stroke patients. Neurology. 2010;75:2176–2184. doi: 10.1212/WNL.0b013e318202013a [PubMed: 21068427]
14. Corbetta M, Kincade MJ, Lewis C, Snyder AZ, Sapir A. Neural basis and recovery of spatial attention deficits in spatial neglect. Nat Neurosci. 2005;8:1603–1610. doi: 10.1038/nnl574 [PubMed: 16234807]
15. He BJ, Snyder AZ, Vincent JL, Epstein A, Shulman GL, Corbetta M. Breakdown of functional connectivity in frontoparietal networks underlies behavioral deficits in spatial neglect. Neuron. 2007;53:905–918. doi: 10.1016/j.neuron.2007.02.013 [PubMed: 17359924]

16. Carter AR, Astafiev SV, Lang CE, Connor LT, Rengachary J, Strube MJ, et al. Resting interhemispheric functional magnetic resonance imaging connectivity predicts performance after stroke. Ann Neurol. 2010;67:365–375. doi: 10.1002/ana.21905 [PubMed: 20373348]
17. Dacosta-Aguayo R, Graña M, Iturria-Medina Y, Fernández-Andújar M, López-Cancio E, Cáceres C, et al. Impairment of functional integration of the default mode network correlates with cognitive outcome at three months after stroke. Hum Brain Mapp. 2015;36:577–590. doi: 10.1002/hbm.22648 [PubMed: 25324040]
18. Park JY, Kim YH, Chang WH, Park CH, Shin YI, Kim ST, et al. Significance of longitudinal changes in the default-mode network for cognitive recovery after stroke. Eur J Neurosci. 2014;40:2715–2722. doi: 10.1111/ejn.12640 [PubMed: 24931140]
19. Dacosta-Aguayo R, Graña M, Savio A, Fernández-Andújar M, Millán M, López-Cancio E, et al. Prognostic value of changes in resting-state functional connectivity patterns in cognitive recovery after stroke: A 3T fMRI pilot study. Hum Brain Mapp. 2014;35:3819–3831. doi: 10.1002/hbm.22439 [PubMed: 24523262]
20. Ding X, Li CY, Wang QS, Du FZ, Ke ZW, Peng F, et al. Patterns in default-mode network connectivity for determining outcomes in cognitive function in acute stroke patients. Neuroscience. 2014;277:637–646. doi: 10.1016/j.neuroscience.2014.07.060 [PubMed: 25090922]
21. Tuladhar AM, Snaphaan L, Shumskaya E, Rijpkema M, Fernandez G, Norris DG, et al. Default mode network connectivity in stroke patients. PLoS One. 2013;8:e66556. doi: 10.1371/journal.pone.0066556 [PubMed: 23824302]
22. Feng W, Wang J, Chhatbar PY, Doughty C, Landsittel D, Lioutas VA, et al. Corticospinal tract lesion load: an imaging biomarker for stroke motor outcomes. Ann Neurol. 2015;78:860–870. doi: 10.1002/ana.24510 [PubMed: 26289123]
23. Almeida SR, Vicentini J, Bonilha L, De Campos BM, Casseb RF, Min LL. Brain connectivity and functional recovery in patients with ischemic stroke. J Neuroimaging. 2017;27:65–70. doi: 10.1111/jon.l2362 [PubMed: 27244361]
24. Lokeskrawee T, Muengtaweepongsa S, Patumanond J, Tiamkao S, Thamangraksat T, Phankhian P, et al. Prediction of symptomatic intracranial hemorrhage after intravenous thrombolysis in acute ischemic stroke: the symptomatic intracranial hemorrhage score. J Stroke Cerebrovasc Dis. 2017;26:2622–2629. doi: 10.1016/j.jstrokecerebrovasdis.2017.06.030 [PubMed: 28826584]
25. Brott T, Adams HP Jr, Olinger CP, Marier JR, Barsan WG, Biller J, et al. Measurements of acute cerebral infarction: a clinical examination scale. Stroke. 1989;20:864–870. [PubMed: 2749846]
26. Suiter G, Steen C, De Keyser J. Use of the Barthel index and modified Rankin scale in acute stroke trials. Stroke. 1999;30:1538–1541. [PubMed: 10436097]
27. Prabhakaran S, Ruff I, Bernstein RA. Acute stroke intervention: a systematic review. JAMA. 2015;313:1451–1462. doi: 10.1001/jama.2015.3058 [PubMed: 25871671]
28. de Haan B, Clas P, Juenger H, Wilke M, Karnath HO. Fast semi-automated lesion demarcation in stroke. Neuroimage Clin. 2015;9:69–74. doi: 10.1016/j.nicl.2015.06.013 [PubMed: 26413473]
29. Song XW, Dong ZY, Long XY, Li SF, Zuo XN, Zhu CZ, et al. REST: a toolkit for resting-state functional magnetic resonance imaging data processing. PLoS One. 2011;6:e25031. doi: 10.1371/joumal.pone.0025031 [PubMed: 21949842]
30. Mazziotta J, Toga A, Evans A, Fox P, Lancaster J, Zilles K, et al. A four-dimensional probabilistic atlas of the human brain. J Am Med Inform Assoc. 2001;8:401–430. [PubMed: 11522763]
31. Desikan RS, Ségonne F, Fischl B, Quinn BT, Dickerson BC, Blacker D, et al. An automated labeling system for subdividing the human cerebral cortex on MRI scans into gyral based regions of interest. Neuroimage. 2006;31:968–980. doi: 10.1016/j.neuroimage.2006.01.021 [PubMed: 16530430]
32. Zhu SC, Yuille A. Region competition: unifying snakes, region growing, and Bayes/MDL for multiband image segmentation. IEEE Trans Pattern Anal Mach Inteil. 1996; 18,884–900.
33. Mantas J Classification methods. Stud Health Technol Inform. 2002;65:148–163. [PubMed: 15460225]
34. Van Hoesen GW, Pandya DN, Butters N. Cortical afferents to the entorhinal cortex of the Rhesus monkey. Science. 1972;175:1471–1473. [PubMed: 4622430]

35. Van Hoesen GW, Pandya DN. Some connections of the entorhinal (area 28) and perirhinal (area 35) cortices of the rhesus monkey. III. Efferent connections. Brain Res. 1975;95:39–59. [PubMed: 1156868]
36. Lacruz ME, García Seoane JJ, Valentin A, Selway R, Alarcón G. Frontal and temporal functional connections of the living human brain. Eur J Neurosci. 2007;26:1357–1370. doi: 10.1111/j.l460-9568.2007.05730.x [PubMed: 17767512]
37. van Meer MP, van der Marel K, Otte WM, Berkelbach van der Sprenkel JW, Dijkhuizen RM. Correspondence between altered functional and structural connectivity in the contralesional sensorimotor cortex after unilateral stroke in rats: a combined resting-state functional MRI and manganese-enhanced MRI study. J Cereb Blood Flow Metab. 2010;30:1707–1711. doi: 10.1038/jcbfm.2010.124 [PubMed: 20664609]
38. Pani E, Zheng X, Wang J, Norton A, Schlaug G. Right hemisphere structures predict poststroke speech fluency. Neurology. 2016;86:1574–1581. doi: 10.1212/WNL.0000000000002613 [PubMed: 27029627]
39. Wu J, Quinlan EB, Dodakian L, McKenzie A, Kathuria N, Zhou RJ, et al. Connectivity measures are robust biomarkers of cortical function and plasticity after stroke. Brain.2015;138:2359–2369. [PubMed: 26070983]
40. Wang L, Yu C, Chen H, Qin W, He Y, Fan F, et al. Dynamic functional reorganization of the motor execution network after stroke. Brain. 2010; 133(pt 4): 1224–1238. doi: 10.1093/brain/awq043 [PubMed: 20354002]
41. Park CH, Chang WH, Ohn SH, Kim ST, Bang OY, Pascual-Leone A, et al. Longitudinal changes of resting-state functional connectivity during motor recovery after stroke. Stroke. 2011;42:1357–1362. doi: 10.1161/STROKEAHA.110.596155 [PubMed: 21441147]
42. Demuru M, van Duinkerken E, Fraschini M, Marrosu F, Snoek FJ, Barkhof F, et al. Changes in MEG resting-state networks are related to cognitive decline in type 1 diabetes mellitus patients. Neuroimage Clin. 2014;5:69–76. doi: 10.1016/j.nicl.2014.06.001 [PubMed: 25003029]
43. Prabhakaran S, Zarahn E, Riley C, Speizer A, Chong JY, Lazar RM, et al. Inter-individual variability in the capacity for motor recovery after ischemic stroke. Neurorehabil Neural Repair. 2008;22:64–71. doi: 10.1177/1545968307305302 [PubMed: 17687024]
44. Coupar F, Pollock A, Rowe P, Weir C, Langhome P. Predictors of upper limb recovery after stroke: a systematic review and meta-analysis. Clin Rehabil. 2012;26:291–313. doi: 10.1177/0269215511420305 [PubMed: 22023891]
45. Koh CL, Pan SL, Jeng JS, Chen BB, Wang YH, Hsueh IP, et al. Predicting recovery of voluntary upper extremity movement in subacute stroke patients with severe upper extremity paresis. PLoS One. 2015;10:e0126857. doi: 10.1371/journal.pone.0126857 [PubMed: 25973919]
46. Triantafyllou C, Hoge RD, Krueger G, Wiggins CJ, Potthast A, Wiggins GC, et al. Comparison of physiological noise at 1.5 T, 3 T and 7 T and optimization of fMRI acquisition parameters. Neuroimage. 2005;26:243–250. doi: 10.1016/j.neuroimage.2005.01.007 [PubMed: 15862224]
47. Chen W, Ugurbil K. High spatial resolution functional magnetic resonance imaging at very-high-magnetic field. Top Magn Reson Imaging. 1999;10:63–78. [PubMed: 10389673]
48. Stefanovic Budimkic M, Pekmezovic T, Beslac-Bumbasirevic L, Ercegovac M, Berisavac I, Stanarcevic P, et al. Long-term prognosis in ischemic stroke patients treated with intravenous thrombolytic therapy. J Stroke Cerebrovasc Dis. 2017;26:196–203. doi: 10.1016/j.jstrokecerebrovasdis.2016.09.009 [PubMed: 28341074]

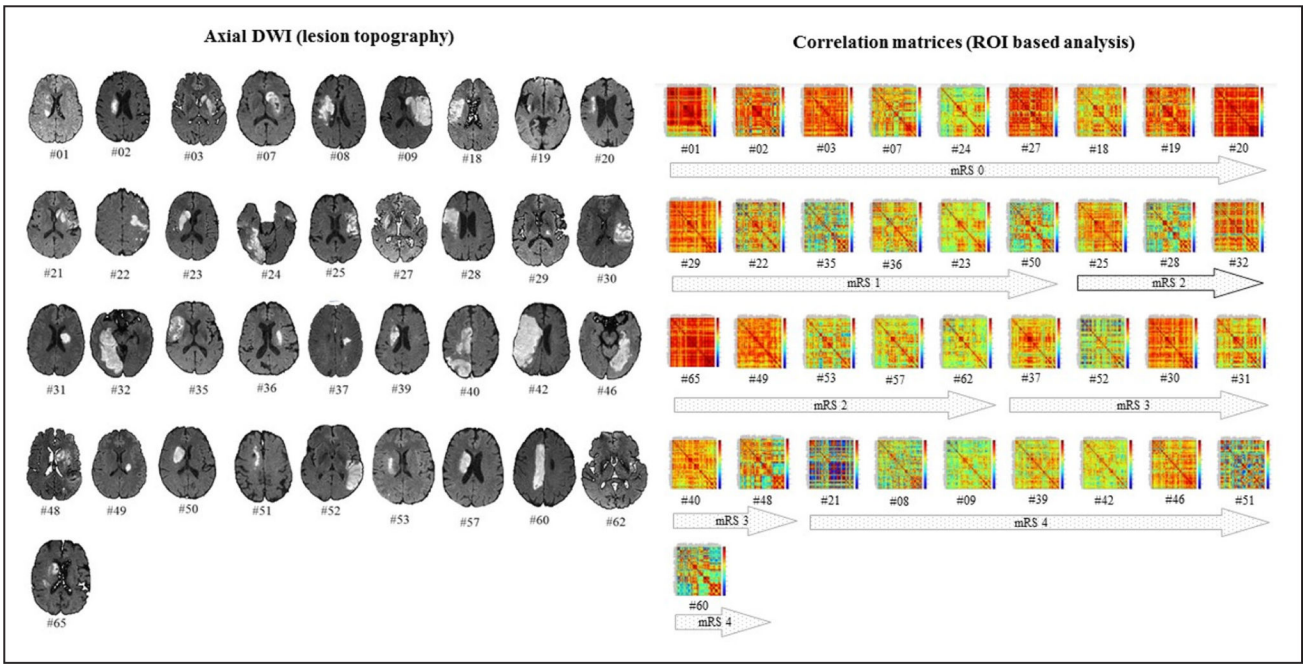

Figure 1.

Infarct lesions and region of interest (ROI)-based analysis for all patients included in the study according to the functional outcome at 90 d. The **right** displays the correlation coefficient weighted matrices for every pairwise region. DWI indicates diffusion weighted imaging; and mRS, modified Rankin Scale.

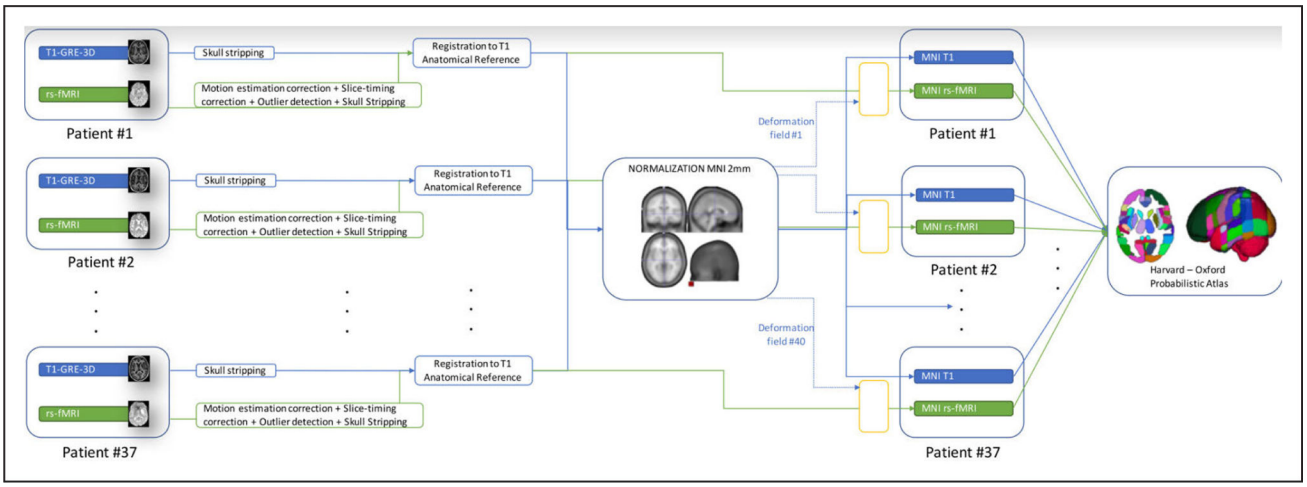

Figure 2.

Preprocessing flowchart. GRE-3D indicates gradient-recalled echo tridimensional; MNI, Montreal Neurological Institute; and rs-fMRI, resting-state functional magnetic resonance imaging.

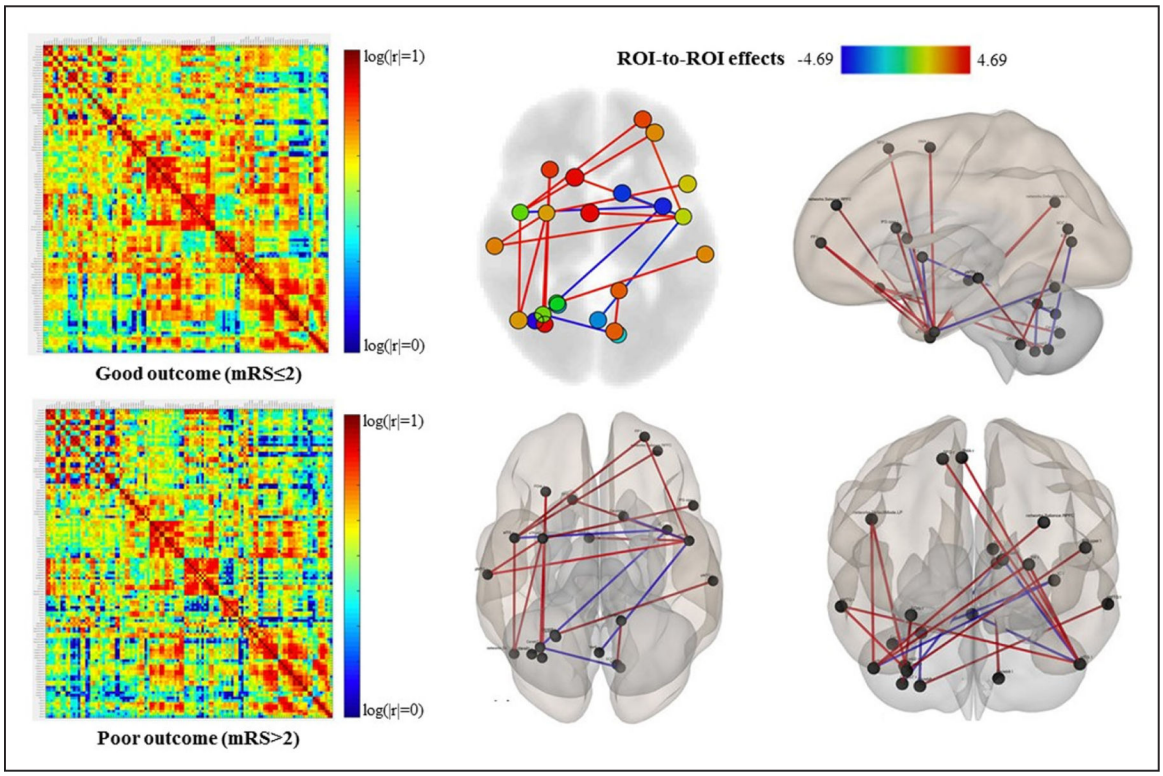

Figure 3.

Regions of interest (ROI)-based analysis for patients with good (modified Rankin Scale [mRS] ≤2) and poor (mRS >2) functional outcome. **Left** display the correlation coefficients matrices for every pairwise region. Red areas indicate stronger functional connections between regions, whereas blue areas indicate a low correlation between regions. Patients with good outcome there are mainly yellow to red areas, whereas in patients with poor outcome these are not so intense and have lower values of connectivity. The **right** display the graph visualization of the mean correlation coefficient weighted matrices for the group of patients with good outcome at 90 d, thresholded at ***P***<0.05.

Table 1.

Demographic and Clinical Data

Characteristics	Overall (n=37)	Good Outcome (mRS 0–2; n=23)	Poor Outcome (mRS 3–4;n=14)	*P* Value
Age, median (IQR)	72 (58–81)	70 (53–80)	76 (64–82)	0.266
Sex (male:female)	23:14	17:6	6:8	0.059
Alcohol intake	10.8	8.7	14.3	0.595
Smoking	35.1	39.1	28.6	0.514
Hypertension	75.7	78.3	71.4	0.639
Diabetes mellitus	18.9	17.4	21.4	0.761
Dyslipemia	51.4	60.9	35.7	0.138
NIHSS at admission, median (IQR)	12 (5–17)	11 (5–15)	16 (5–17)	0.292
3 d-NIHSS, median (IQR)	4 (2–8)	3 (1–4)	8 (5–13)	<0.001
Infarct volume, mean (IQR), mL	20.2 (5.4–38.3)	14.7 (5.7–26.6)	28.5 (9.1–56.1)	0.147
Laterality (right/left/both), %	51.4/40.5/8.1	52.2/43.5/4.3	50/35.7/14.3	0.550
Frontal lobe affected, %	58.3	54.5	64.3	0.563
Temporal lobe affected, %	30.6	22.7	42.9	0.201
Parietal lobe affected, %	25	18.2	35.7	0.236
Occipital lobe affected, %	16.7	13.6	21.4	0.541
Corona radiata affected, %	41.7	40.9	42.9	0.908
Thalamus affected, %	11.1	13.6	7.1	0.546
Caudate affected, %	50	45.5	57.1	0.494
Lentiform nucleus affected, %	52.8	50	57.1	0.676
Insular cortex affected, %	50	59.1	35.7	0.171
Middle cerebral artery territory, %	83.3	90.0	71.4	0.126
Anterior cerebral artery territory, %	8.3	0	21.4	0.023
Posterior cerebral artery territory, %	13.9	9.1	21.4	0.297
Time to symptom onset to r-tPA administration, median (IQR)	172 (130–250)	159 (125–190)	190 (150–260)	0.361
Hemorrhagic transformation (HI1/HI2/PH1), %	8.1/10.8/2.7	4.3/4.3/4.3	14.3/21.4/0	0.205
Mechanical thrombectomy, %	13.5	21.7	0	0.061
90 d-NIHSS, median (IQR)	1 (0–3)	0(0–1)	3 (2–5)	0.007

HI indicates hemorrhagic infarction; IQR, interquartile range; mRS, modified Rankin Scale; NIHSS, National Institutes of Health Stroke Scale; PH, parenchymal hematoma; and r-tPA, recombinant tissue-type plasminogen activator.

Table 2.

Significant Functional Connectivity ROI-to-ROI Relationships

Regions	T Statistic	*P* Value-Uncorrected	False-Discovery Rate (P-FDR)
Right lateral parietal; right anterior temporal fusiform cortex	4.69	0.0001	0.011
Left supracalcarine cortex; left cerebellum 9	4.35	0.0002	0.027
Right anterior inferior temporal gyrus; left frontal superior gyrus	4.00	0.0004	0.033
Left anterior inferior temporal gyrus; right supplementary motor cortex	3.88	0.0006	0.041
Right anterior inferior temporal gyrus; salience network rostrolateral prefrontal cortex	3.84	0.0006	0.033
Right anterior temporal fusiform cortex; left inferior frontal gyrus, pars opercularis	3.83	0.0007	0.049
Right anterior inferior temporal gyrus; right lateral parietal	3.75	0.0008	0.033
Right anterior temporal fusiform cortex; right middle temporal gyrus, posterior division	3.71	0.0009	0.049
Left anterior inferior temporal gyrus; right middle temporal gyrus, posterior division	3.69	0.0010	0.041
Left anterior inferior temporal gyrus; right frontal superior gyrus	3.67	0.0010	0.041
Left anterior inferior temporal gyrus; vermis 6	−3.59	0.0013	0.041
Left anterior inferior temporal gyrus; left caudate	−3.85	0.0006	0.041
Right cerebellum crus 1; left insular cortex	−3.95	0.0005	0.039
Left insular cortex; right anterior inferior temporal gyrus	−4.14	0.0003	0.040
Right cerebellum 7b; left intracalcarine cortex	−4.48	0.0001	0.019

P-FDR indicates ***P*** value-false discovery rate; and ROI, region of interest.

Table 3.

Results of Canonical Discriminant Analysis: Loadings of Correlation Matrix Between Predictor Variables (Standardized Canonical Coefficients) and Discriminant Function

Predictor Variables	Standardized Canonical Discriminant Function Coefficients
Age	0.386
3 d-NIHSS	0.849
Infarct volume	−0.362
Right anterior inferior temporal gyrus and left superior frontal medial cortex	1.682
Left anterior inferior temporal gyrus and right superior frontal gyrus	−1.325
Left anterior inferior temporal gyrus and left caudate	−1.300
Right anterior temporal fusiform cortex and left inferior frontal gyrus, pars opercularis	0.381
Right anterior temporal fusiform cortex and right middle temporal gyrus, posterior division	0.478
Left insular cortex and right cerebellum crus 1	0.479
Left insular cortex and right anterior inferior temporal gyrus	−0.353
Right cerebellum 7b and left intracalcarine cortex	−0.310
Left supracalcarine cortex and left cerebellum 9	0.373

NIHSS indicates National Institutes of Health Stroe Scale.